Suppressed electric quadrupole moment of thulium atomic clock states

Timo Fleig*
Laboratoire de Chimie et Physique Quantiques, FeRMI, Université Paul Sabatier Toulouse III, 118 Route de Narbonne, F-31062 Toulouse, France

(Received 6 February 2023; accepted 9 March 2023; published 16 March 2023)

A method for highly accurate calculations of atomic electric quadrupole moments (EQM) is presented, using relativistic general-excitation-rank configuration interaction wave functions based on Dirac spinors. Application to the clock transition states of the thulium atom employing up to full Quadruple excitations for the atomic wave function yields a final value of $Q_{zz}(^2F_{7/2}) = 0.07^{+0.07}_{-0.00}$ *a.u.*, establishing that the thulium electronic ground state has an exceptionally small EQM. A detailed analysis of this result is presented which has implications for EQMs of other atoms with unpaired f electrons.

DOI: 10.1103/PhysRevA.107.032816

I. INTRODUCTION

In atomic systems electric quadrupole moments of the electron shells are of importance in the quest for setting new standards of time measurement. In fact, they are often one of the limiting quantities in optical atomic clock's fractional frequency uncertainty [1]. The reason for this type of uncertainty is that, in many implementations of atomic clocks an environmental perturbation, a residual external electric-field gradient interacts with the electric quadrupole moments (EQM) of the (atomic) charge distribution in the relevant clock-transition states, giving rise to the so-called "quadrupole shifts" [2] of atomic energy levels.

Lanthanide atoms have electronic valence shells $4f^k$ where the k f electrons are partially shielded from external electric fields by the electrons occupying the $6s$ shell. This makes f–f transitions in lanthanides less susceptible to EQM interactions with the gradients of an external electric field [3]. Indeed, great progress has very recently been made in devising a transportable optical clock using the hyperfine levels of the ground-state f–f transition in thulium atoms [4–7]. The EQM interaction is nevertheless one of the sources of uncertainty in this type of atomic clock. However, electronic properties of lanthanide atoms are notoriously difficult to calculate accurately.

The method of calculating EQMs presented in this paper is based on relativistic configuration interaction (CI) wave functions of general excitation rank, up to the level of Full CI [8]. The implementation is highly efficient, allowing for CI expansions with up to 10^{10} (10 billion) linear expansion terms and thus for very accurate calculation of electron correlation effects. This will be demonstrated in the present paper. Moreover, the present approach is particularly advantageous when atomic states with complicated shell structure, such as with several unpaired d and/or f electrons, have to be addressed [9]. The present approach is also directly applicable to molecules.

The article is structured as follows. In Sec. II the theory of the atomic electric quadrupole moment is briefly reviewed and the present implementation using relativistic configuration interaction (CI) wave functions for electronic ground and excited states is described. The same method is in the present also applied in the calculation of the magnetic hyperfine interaction constant. Section III contains the applications, first to the beryllium (Be) atom as a test system for verification of the present implementation, then to the radium monocation (Ra^+) as a more complex system where relativistic effects are strong. Finally, predictions are made for EQMs of ground and excited states of the thulium (Tm) atom. In the final section, Sec. IV, conclusions from the present findings are drawn.

II. THEORY

A. Interaction energy

An arbitrary charge distribution immersed in an external electric field $\mathbf{E}$ gives rise to an electrostatic interaction energy [10], the second-order term of which is written out as

$$W_2 = -\frac{1}{6}\sum_{i,j} Q_{ij}\left.\frac{\partial E_j(\mathbf{x})}{\partial x_i}\right|_{\mathbf{x}=\mathbf{x}_0}, \tag{1}$$

where $\mathbf{x}_0$ is an appropriately chosen expansion point, $\mathbf{Q}$ is the rank-2 electric quadrupole moment tensor of the charge distribution, and $\frac{\partial E_j(\mathbf{x})}{\partial x_i}$ is a component of the electric-field gradient. In the present case, the charge distribution is represented by the electron shells of the atomic systems under consideration. The atomic nucleus is described by a spherical Gaussian charge distribution and thus does not contribute to the EQM of the atom.

B. Atomic electric quadrupole moment

The relevant element of the rank-2 tensor Q of the atomic electric quadrupole moment has been defined as [2,11,12], in a.u.,

$$Q_{zz} := \langle\Psi| - \sum_{i=1}^{n}\sqrt{\frac{4\pi}{5}}\, r^2(i)\, Y_{2,0}(\vartheta,\varphi)|\Psi\rangle, \tag{2}$$

*timo.fleig@irsamc.ups-tlse.fr

with Ψ the atomic wave function, n the number of electrons, r the radial electron coordinate, and Y_{ℓ,m_ℓ} a spherical harmonic. In the Condon-Shortley convention we have

$$Y_{2,0}(\vartheta,\varphi) = \frac{1}{4}\sqrt{\frac{5}{\pi}}\,(3\cos^2(\vartheta)-1). \tag{3}$$

Therefore,

$$Q_{zz} = -\frac{1}{2}\,\langle\Psi|\sum_{i=1}^{n} r^2(i)\,(3\cos^2(\vartheta)-1)|\Psi\rangle. \tag{4}$$

An elementary coordinate transformation yields

$$r^2\,(3\cos^2(\vartheta)-1) = 2z^2 - x^2 - y^2, \tag{5}$$

in terms of cartesian coordinates, and so

$$\begin{aligned} Q_{zz} &= -\frac{1}{2}\,\langle\Psi|\sum_{i=1}^{n}(2z^2(i)-x^2(i)-y^2(i))|\Psi\rangle \\ &= -\frac{1}{2}\left\{\langle\Psi|\sum_{i=1}^{n}2z^2(i)|\Psi\rangle - \langle\Psi|\sum_{i=1}^{n}x^2(i)|\Psi\rangle \right. \\ &\quad \left. - \langle\Psi|\sum_{i=1}^{n}y^2(i)|\Psi\rangle\right\}. \end{aligned} \tag{6}$$

The tensor element is evaluated by calculating the three resulting matrix elements over cartesian one-electron operators, the "second moments." In the present case, however, $|\Psi\rangle \equiv |\alpha\,J\,M_J\rangle$ is a relativistic atomic wave function where α represents quantum numbers other than the total angular momentum J. Since a linear symmetry double group (in the present case D^*_{32h}, which is an abelian subgroup of $D^*_{\infty h}$) is used instead of full rotational atomic symmetry the wave functions are obtained for individual M_J states. In practice, J for a given eigenvector is inferred by calculating a sufficient number of degenerate eigenvectors in the different relevant M_J subspaces. The individual states are represented by relativistic configuration interaction wave functions

$$|\alpha\,J\,M_J\rangle \equiv \sum_{I=1}^{\dim\mathcal{F}^t(\mathrm{M,n})} c_{(\alpha,J,M_J),I}\,(\mathcal{S}\overline{\mathcal{T}})_I|\rangle, \tag{7}$$

where $\mathcal{F}^t(M,n)$ is the symmetry-restricted sector of Fock space with n electrons in M four-spinors, $\mathcal{S} = a_i^\dagger a_j^\dagger a_k^\dagger \ldots$ is a string of spinor creation operators, $\overline{\mathcal{T}} = a_{\bar{l}}^\dagger a_{\bar{m}}^\dagger a_{\bar{n}}^\dagger \ldots$ is a string of creation operators of time-reversal transformed spinors. The determinant expansion coefficients $c_{(\alpha,J,M_J),I}$ are generally obtained as described in Refs. [13,14] by diagonalizing the Dirac-Coulomb Hamiltonian (in a.u.)

$$\begin{aligned} \hat{H}^{\text{Dirac-Coulomb}} &= \sum_j^n \left[c\,\boldsymbol{\alpha}_j\mathbf{p}_j + \beta_j c^2 - \frac{Z}{r_j}\mathbb{1}_4\right] \\ &\quad + \sum_{j,k>j}^{n}\frac{1}{r_{jk}}\mathbb{1}_4 \end{aligned} \tag{8}$$

in the basis of the states $(\mathcal{S}\overline{\mathcal{T}})_I|\,\rangle$, where the indices j,k run over electrons, Z is the proton number, and $\boldsymbol{\alpha}$, β are standard Dirac matrices. Reference states and spinors for correlated many-body calculations are obtained in the independent-particle picture using the Dirac-Coulomb Hamiltonian and are abbreviated Dirac-Coulomb Hartree-Fock (DCHF). The framework for the present implementation is the relativistic electronic-structure program package DIRAC [15] where a locally modified version of the code is used.

In the present paper the electric quadrupole tensor component is evaluated for the microstate with $M_J = J$, i.e.,

$$Q_{zz} = -\frac{1}{2}\,\langle\alpha\,J\,J|\sum_{i=1}^{n}(2z^2(i)-x^2(i)-y^2(i))|\alpha\,J\,J\rangle, \tag{9}$$

based on the evaluation of properties using relativistic CI wave functions as described in Refs. [8,16]. From the EQM expectation value for a given eigenvector with defined M_J the EQM for the other M_J components of the associated state J can be calculated via the reduced matrix element (RME) evaluated through the adapted form of the Wigner-Eckhart theorem

$$\mathrm{RME} = \langle\alpha\,J||\hat{Q}_{zz}||\alpha\,J\rangle = \frac{\langle\alpha\,J\,M_J|\hat{Q}_{zz}|\alpha\,J\,M_J\rangle\,\sqrt{2J+1}}{\langle J\,2\,M_J\,0|J\,2\,J\,M_J\rangle}, \tag{10}$$

where $\hat{Q}_{zz} = -\frac{1}{2}\sum_{i=1}^{n}[2z^2(i)-x^2(i)-y^2(i)]$ and α denotes quantum numbers other than those of total electronic angular momentum J. The Clebsch-Gordan coefficients (CGC) in the denominator of Eq. (10) are calculated according to Wigner's (1959) general definition [17] as given in Ref. [18]

$$\begin{aligned} &\langle j_1 j_2 m_{j_1} m_{j_2}|j_1 j_2 j m_j\rangle \\ &= \delta(m_j, m_{j_1}+m_{j_2})\sqrt{\frac{(j_1+j_2-j)!(j+j_1-j_2)!(j+j_2-j_1)!(2j+1)}{(j+j_1+j_2+1)!}} \\ &\quad\times\sum_k \frac{(-1)^k\sqrt{(j_1+m_{j_1})!(j_1-m_{j_1})!(j_2+m_{j_2})!(j_2-m_{j_2})!(j+m_j)!(j-m_j)!}}{k!(j_1+j_2-j-k)!(j_1-m_{j_1}-k)!(j_2+m_{j_2}-k)!(j-j_2+m_{j_1}+k)!(j-j_1-m_{j_2}+k)!}. \end{aligned} \tag{11}$$

C. Magnetic hyperfine interaction

The magnetic hyperfine interaction constant was implemented in the present electronic-structure methods as described in Refs. [19,20]. For n electrons in the field of the atomic nucleus it is defined in a.u. as

$$A = -\frac{\mu[\mu_N]}{2cIm_pM_J}\,\langle J\,M_J|\sum_{i=1}^{n}\left(\frac{\boldsymbol{\alpha}_i\times\mathbf{r}_i}{r_i^3}\right)_z|J\,M_J\rangle, \tag{12}$$

where μ is the nuclear magnetic moment, $\frac{1}{2cm_p}$ is the nuclear magneton in a.u., m_p is the proton rest mass, I is the nuclear spin quantum number, and $\mathbf{r}$ is the electron position operator.

III. APPLICATIONS AND RESULTS

A. Be

1. Technical details

The Gaussian basis set for Be is cc-pV6Z with added diffuse functions from the set aug-cc-pV5Z [21], amounting to $\{17s, 10p, 6d, 5f, 4g, 3h, 1i\}$ uncontracted functions. Spinors are optimized for the closed-shell ground state ($1s^2 2s^2$). A cutoff energy of 100 a.u. is used for the virtual spinor set. A full CI expansion is used which includes the entire set of triple and quadruple excitations, amounting to ≈29 million Slater determinants.

2. Results and discussion

The above-defined model yields $Q_{zz}(2s^1 2p^1; {}^3P_2) = 2.2721$ a.u. for this Be-excited state. For comparison, the four-electron limit result from Ref. [11] is $Q_{zz}(2s^1 2p^1; {}^3P_2) = 2.265$ a.u. This differs from the present result by only roughly 0.3% confirming the reliability of the present implementation. The small difference is not explained by relativistic effects which were found to be smaller than 0.01%, but rather by the fact that in Ref. [11] a finite-element method was used whereas, in the present case, a finite Gaussian basis set is employed.

As a further consistency test $Q_{zz}(2s^1 2p^1; {}^3P_2, M_J = 1) = -1.136$ a.u. is calculated explicitly from the relevant M_J eigenvector. The value for $Q_{zz}(2s^1 2p^1; {}^3P_2, M_J = 1)$ but calculated from $Q_{zz}(2s^1 2p^1; {}^3P_2, M_J = 2)$ and $\mathrm{RME}(2s^1 2p^1; {}^3P_2)$ obtained from Eq. (10) is indeed identical.

B. Ra^+

1. Technical details

For Ra^+ a Gaussian basis set of quadruple-zeta quality is used where all $\{6s, 6p, 7s, 7p\}$-correlating and all dipole-polarizing primitive functions were included [22]. The Dirac spinors are optimized by diagonalizing a Fock operator where a fractional occupation of $f = \frac{1}{12}$ per $7s$ and $6d$ spinor is used. Effectively, this yields a Dirac-Hartree-Fock state that is averaged over the ${}^2S_{1/2}$ ground term and the ${}^2D_{3/2,5/2}$ excited terms with spinors that are not biased towards any of the corresponding states.

Acronyms are used for brevity in defining atomic correlated wave functions, also in the following section on the Tm atom. As an example, SDT9_10 a.u. stands for single, double, triple replacements relative to the DCHF reference state where the outermost nine electrons (occupying the shells $6s, 6p, 7s$ in the DCHF reference state) are described by the correlation expansion and the space of virtual spinors is truncated at 10 a.u.

2. Results and discussion

EQMs and level energies for Ra^+ are compiled in Table I. The DCHF results using spinors specific to the electronic ground state of Ra^+ ($7s^1$ configuration) exhibit large deviations from the experiment and from reliable theoretical results. The spinor averaging [DCHF (av.)] rectifies this problem to a large degree. Including electron correlation effects at up to the level of Double excitations (model SD9_10 a.u.) based on the state-averaged spinors diminishes $Q_{zz}({}^2D_{3/2})$ by roughly 10% and $Q_{zz}({}^2D_{5/2})$ by 8%, respectively. Triple excitations are also not unimportant, further quenching $Q_{zz}({}^2D_{3/2})$ and $Q_{zz}({}^2D_{5/2})$ by 3–4%. The term energies for both excited states are in excellent agreement with the experiment in the most accurate model, SDT9_10 a.u., where deviations are less than 1%. Present uncertainties are estimated conservatively to be at most as large as the effect of triple excitations, accounting for excitation ranks higher than triples and basis-set truncations.

TABLE I. Atomic electric quadrupole moments and level energies for state k, defined as $\Delta\varepsilon(k) = \varepsilon(k) - \varepsilon({}^2S_{1/2})$ with ε the total electronic energy, for Ra^+.

Excited state	CI model	$\Delta\varepsilon$ [cm^{-1}]	Q_{zz} [a.u.]
${}^2D_{3/2}(3d^1)$	DCHF ($7s^1$)	15295	4.944
	DCHF (av.)	13053	3.312
	SD9_10au	12171	2.998
	SDT9_10au	12083	2.879
	Final	**12083**	**2.88(12)**
	Other theory		2.84(3) [23]
			2.90(2) [24]
	Exp. [25]	12084.3	
${}^2D_{5/2}(3d^1)$	DCHF ($7s^1$)	16021	7.309
	DCHF (av.)	13853	4.964
	SD9_10au	13639	4.559
	SDT9_10au	13654	4.402
	Final	**13654**	**4.40(16)**
	Other Theory		4.34(4) [23]
			4.45(9) [24]
	Exp. [25]	13 743.0	

The present final results fall in between those from Refs. [23] and [24] and are, considering uncertainties, compatible with both. However, from the present series of calculations, it can be concluded that quadruple excitations and beyond will lead to a further, albeit small, downward correction to Q_{zz}, likely on the order of 1–2%. A further downward correction of a few percent is to be expected from the inclusion of basis functions with high angular momentum ($\ell > 4$), as was pointed out in Refs. [23,26]. The present basis set terminates at $\ell = 4$ for the large-component of the four-component wave functions. Thus, the present EQM results for Ra^+ are in very good agreement with those from Ref. [23] which remain the most accurate to date. This is a further confirmation of the reliability of the present approach to calculating atomic EQMs, which was the goal for this study on Ra^+.

C. Tm

The afore-going sections have set the stage for making reliable predictions for EQMs in systems where they are so far unknown.

TABLE II. Atomic electric quadrupole moments for Tm $^2F_{7/2}(4f^{13}\,6s^2)$ using various CI models, TZ basis.

CI model (number of virtual functions)	Q_{zz} [a.u.]
DCHF	−0.2711
SD15_0.2 a.u. ($1s$, $1d$; $2p$)	0.1128
SD15_1 a.u. ($2s$, $3d$, $1g$; $3p$, $2f$)	−0.0101
SD15_2 a.u. ($3s$, $4d$, $2g$; $4p$, $3f$)	−0.1170
SD15_4 a.u. ($3s$, $4d$, $2g$; $4p$, $4f$, $1h$)	−0.1920
SD15_6 a.u. ($4s$, $5d$, $2g$; $5p$, $5f$, $1h$)	−0.2319
SD15_10 a.u. ($4s$, $6d$, $3g$; $5p$, $6f$, $1h$)	−0.2519
SD15_20 a.u. ($5s$, $7d$, $3g$; $6p$, $7f$, $1h$)	−0.2543
SD15_50 a.u. ($6s$, $8d$, $4g$; $7p$, $8f$, $2h$)	−0.2530
SD15_130 a.u. ($7s$, $9d$, $4g$; $8p$, $9f$, $2h$)	−0.2531
SD23_10 a.u.	−0.2470
SD33_10 a.u.	−0.2473
SDT15_0.2 a.u.	0.1181
SDT15_1 a.u.	0.0509
SDT15_2 a.u.	−0.0139
SDT15_4 a.u.	−0.0498
SDT15_6 a.u.	−0.0472
SDT15_10 a.u.	−0.0299
SDT15_20 a.u.	−0.0311
SDT15_50 a.u.	−0.0304
SDTQ15_2 a.u.	0.021
SDTQ15_4 a.u.	0.013
SDTQ15_10 a.u. (est.)	0.067

1. Technical details

Two Gaussian basis sets are employed for Tm, Dyall's ccpVTZ set with all $4f$, $6s$, $5s$, $5p$, $5d$-correlating and $4f$ dipole-polarizing functions added amounting to $\{30s, 24p, 18d, 13f, 4g, 2h\}$ functions and Dyall's ccpVQZ set including all valence-correlating and the $4f$ dipole-polarizing functions [27], amounting to $\{35s, 30p, 19d, 16f, 6g, 4h, 2i\}$ functions. The Dirac spinors are optimized by diagonalizing a Fock operator where a fractional occupation of $f = \frac{13}{14}$ per spinor with $\ell = 3$ is used ($4f^{13}\,6s^2$ ground configuration). Effectively, this yields a Dirac-Hartree-Fock state that is averaged over the $^2F_{7/2}$ ground term and the $^2F_{5/2}$ excited term and spinors that are not biased towards any of the corresponding states.

2. Results and discussion

Tables II and III show results for the EQM of the electronic ground term ^2F_J. Valence correlation effects from up to double excitations are converged at the percent level when the virtual spinor space is truncated at 20 a.u. These effects decrease Q_{zz} (on the absolute) by about 6%. However, when full triple excitations are introduced in addition, the EQM is quenched by an astonishing order of magnitude. This strong quenching is basis-set dependent to only about 6%, which justifies a deeper investigation using the smaller TZ basis set only.

The strongest positive contribution to Q_{zz} from excitations into the virtual spinor space is observed at the very low cutoff of 0.2 a.u. Further cutting down on this virtual set reveals that the positive contribution is mainly due to double excitations of the type $6s^2 \rightarrow 5d^2_{5/2,5/2}$, the amplitude (CI coefficient) of which diminishes strongly as the dimension of the virtual space is increased. It is remarkable that the residual quenching of Q_{zz} is about +0.24 a.u. for the model SDT15_20 a.u., which leads to a value for Q_{zz} that is roughly one order of magnitude smaller on the absolute than the DCHF value. Expressed in different terms, we here observe an electron correlation effect (difference between a given CI model and Hartree-Fock theory) of nearly 90%. This extraordinary situation can be attributed to the fact that the open-f-shell contribution to Q_{zz}

TABLE III. Atomic electric quadrupole moments and level energies for state k, defined as $\Delta\varepsilon(k) = \varepsilon(k) - \varepsilon(^2F_{7/2})$ with ε the total electronic energy, for Tm using various CI models, QZ basis.

State	CI model (virtual functions)	$\Delta\varepsilon$ [cm^{-1}]	Q_{zz} [a.u.]
$^2F_{7/2}(4f^{13}\,6s^2)$	DCHF	0	−0.2711
	SD15_10 a.u. ($6s$, $5d$, $4g$, $1i$; $7p$, $7f$, $2h$)	0	−0.2531
	SD15_20 a.u. ($7s$, $6d$, $5g$, $1i$; $8p$, $8f$, $3h$)	0	−0.2546
	SD15_50 a.u. ($8s$, $7d$, $5g$, $2i$; $9p$, $10f$, $3h$)	0	−0.2556
	SDT15_10 a.u.	0	−0.0349
	SDT15_20 a.u.	0	−0.0292
	SDT15_50 a.u.	0	−0.0305
	S8_SD23_10 a.u.	0	−0.2511
	SD23_10 a.u.	0	−0.2534
	Exp. [25]	0	
$^2F_{5/2}(4f^{13}\,6s^2)$	DCHF	9016	−0.2203
	SD15_5 a.u.	9277	−0.1863
	SD15_10 a.u.	9215	−0.2059
	SD15_20 a.u.	9143	−0.2074
	SDT15_20 a.u.	9028	−0.0257
	SD15_50 a.u.	9128	−0.2083
	S8_SD23_10 a.u.	9199	−0.2043
	SD23_10 a.u.	9158	−0.2061
	Exp. [25]	8771.243	

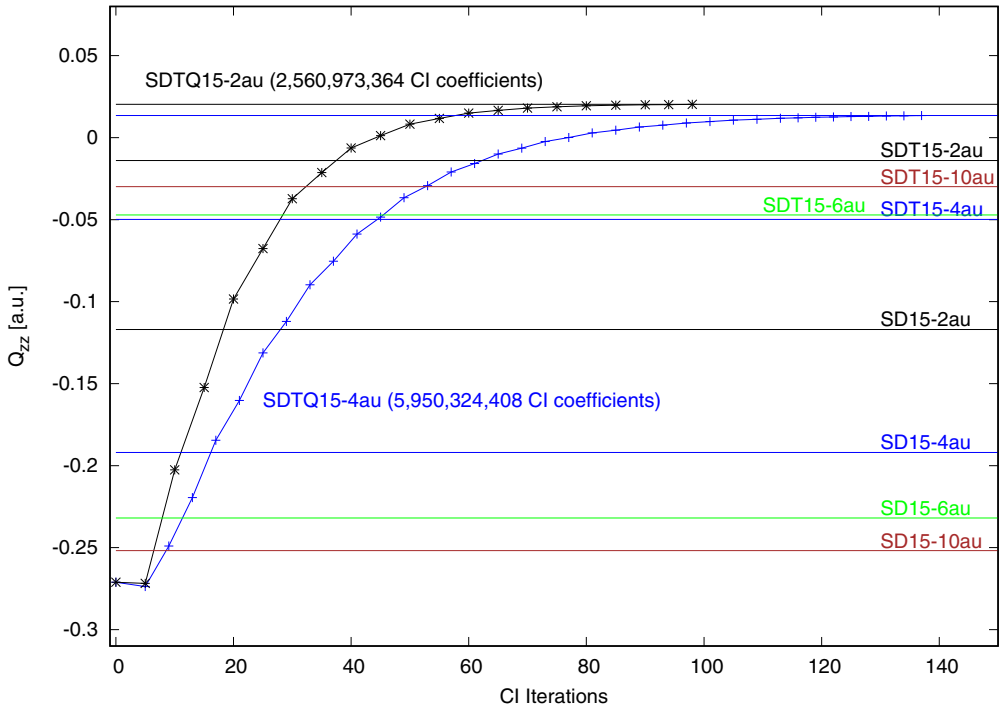

FIG. 1. EQM (a.u.) of $^2F_{7/2}$ Tm ground state using various CI models and virtual cutoffs, TZ basis; horizontal lines display converged values for the respective model. The convergence patterns for the two largest calculations are shown explicitly.

of the thulium atom is rather small and that even a small amplitude on the contributions that arise from d-shell occupations, which, furthermore, have opposite sign, can nearly cancel the latter.

The discussed cancellation leads to values for Q_{zz} that are close to zero and thus manifestly very difficult to describe accurately, i.e., with small relative errors. The inclusion of excitation ranks higher than full triples is explored using the smaller (TZ) basis set, see Table II. Due to the extreme computational demand a truncation of the virtual space has to serve as a further approximation. When this truncation is set to 2 a.u. the difference between the models SDT15 and SDTQ15 is +0.034 a.u. However, with this spinor space the model SDT15 is qualitatively incorrect. A truncation at 4 a.u. yields an SDT15 result that agrees qualitatively with the converged result from SDT15_50 a.u. The corresponding expansion for SDTQ15_4 a.u. comprises roughly six billion expansion terms, close to the limits of computational feasibility with the current code.

A correction due to full quadruple excitations, which is not negligible in the present case, is thus obtained as follows. The base value is provided by the model SDT15_10 a.u. Since correlation contributions at any excitation rank are nearly converged at a virtual cutoff of 10 a.u., but this spinor space creates a configuration space too large to be treated explicitly when Q excitations are taken into account, the result for the model SDTQ15_10 a.u. is estimated by the following formula:

$$\begin{aligned} &Q_{zz}(\text{SDTQ15\_10 a.u.}) \\ &\quad := Q_{zz}(\text{SDT15\_10 a.u.}) + \Delta Q[Q_{zz}(10\,\text{a.u.})] \end{aligned}$$

where

$$\begin{aligned} &\Delta Q[Q_{zz}(10\,\text{a.u.})] \\ &\quad := [Q_{zz}(\text{SDTQ15\_4 a.u.}) - Q_{zz}(\text{SDT15\_4 a.u.})] \\ &\qquad \times \frac{[Q_{zz}(\text{SDT15\_10 a.u.}) - Q_{zz}(\text{SD15\_10 a.u.})]}{[Q_{zz}(\text{SDT15\_4 a.u.}) - Q_{zz}(\text{SD15\_4 a.u.})]}. \end{aligned}$$

This scales the correction due to quadruple excitations by the ratio of the triples correction for different virtual cutoff values. In this estimation the assumption is made that the augmentation of the virtual spinor space affects the triples correction ΔT and the quadruples correction ΔQ in an equivalent manner. This way of obtaining the correction is also supported by the graphical representation in Fig. 1. ΔT is always positive (as is ΔQ) and increases monotonically as a function of virtual cutoff (assumed for ΔQ). Since the correction due to higher excitation ranks is more than halved when going from ΔT to ΔQ a correction $\Delta 5$ due to full quintuples (or to even higher excitation ranks) is not expected to surpass +0.05 a.u. for $Q_{zz}(^2F_{7/2})$.

Possible corrections due to the use of the larger QZ basis set are investigated through the calculations presented in Table III. Interestingly, the most elaborate comparable model SDT15_50 a.u. does not yield a significant basis-set correction (Δ QZ ≈ -0.0001 a.u.). Furthermore, a correction due to core-valence correlation by including single-hole configurations (model S8_SD23_10 a.u.), and in addition, double-hole configurations (model SD23_10 a.u.) in the Tm $5s, 5p$ shells also result in negligibly small corrections. The same is true for correlations due to single- and double-hole configurations in the Tm $4d$ shell (see Table II). The inclusion of additional

functions of very high angular momentum [h ($\ell = 5$) and i ($\ell = 6$)] in the basis set does not affect the EQM of the Tm atom appreciably, as can be seen by comparing the models SDT15_50 a.u. in Tables II and III. Also, the triples correction ΔT increases by only about 2.5% when going from the TZ to the QZ basis, a further indication that many-body effects are well described using the TZ basis set.

The present final best result is, therefore, $\boldsymbol{Q_{zz}(^2F_{7/2}) \approx 0.07}$ a.u. I assign to this a rather conservative (upper) uncertainty of 100%, almost entirely due to the neglect of higher CI excitation ranks in even the most highly correlated atomic wave function (SDTQ). Given the small value of the EQM this uncertainty translates into only 0.07 a.u.

As can be inferred from the above-detailed discussion and the results in Table III it can be said with certainty that $0 < Q_{zz}(^2F_{5/2}) < Q_{zz}(^2F_{7/2})$. This conjecture is supported by the fact that the correlation corrections ΔSD are very similar for the $^2F_{7/2}$ ground state (+0.017 a.u.) and for the excited clock state $^2F_{5/2}$ (+0.013 a.u.). Likewise, the triples corrections ΔT are also similar: +0.225 a.u. and +0.182 a.u. for $^2F_{7/2}$ and $^2F_{5/2}$, respectively. This is not surprising since correlation effects cannot differ greatly between a $4f_{7/2}$-hole and a $4f_{5/2}$-hole atomic configuration, all else being equal. This implies that the quadruples correction ΔQ for the excited clock state is expected to be around +0.08 a.u., inferred from the corrections in Table II, yielding an estimate $Q_{zz}(^2F_{5/2}) \approx$ 0.05 a.u. Thus, the the electronically excited clock state also has suppressed EQM.

The result by Sukachev *et al.* [28] obtained with the COWAN code of $Q_{zz}(^2F_{7/2}) \approx 0.5$ a.u. differs from the present final result by roughly 0.4 a.u. This is a large relative and also a significant absolute difference, given the observed discrepancies from different electronic-structure models as compared for the Ra^+ ion in Sec. III B 2 at the highest level of accuracy. The spread of final values for Ra^+ is about an order of magnitude smaller than 0.4 a.u. Since Sukachev *et al.* did not give any details of their calculation it is not possible to analyze the discrepancy for Tm.

3. Hyperfine interaction

However, a qualitative judgment on the present EQM results is possible in an indirect manner. Since closed-shell contributions to the EQM are zero the spin density in the atomic state is linked to the EQM. The same is true for the magnetic hyperfine interaction constant. Thus, the correlated wave functions presently optimized for the description of the Tm EQM are expected to also describe the corresponding hyperfine interaction constant correctly.

Table IV lists the results for A using wave functions from the most accurate models for calculating the EQM. The spin density in the correlated wave function of the Tm $^2F_{7/2}$ ground state largely resides in f (and d) states which explains why A is comparatively small. Also here the basis set effect is negligibly small. Higher excitations than doubles do not affect A substantially, in contrast to the EQM. This can be understood from the fact that the triples correction as well as higher excitation ranks affect the ratio of spin density in f and d states, thus having a small effect on the hyperfine interaction whereas this change of ratio has a large effect on the EQM. The result with the largest deviation from the experimental value for A is obtained with the model SDT15_50au/QZ which differs from the experimental value by only about 6.8%.

TABLE IV. Magnetic hyperfine interaction constant A for ^{169}Tm $^2F_{7/2}(4f^{13}\,6s^2)$ calculated with Eq. (12) using various CI models and basis sets.

CI model/basis set	A [MHz]
SD15_20 a.u./TZ	−390.2
SDT15_2 a.u./TZ	−388.5
SDT15_4 a.u./TZ	−391.0
SDT15_6 a.u./TZ	−396.8
SDT15_10 a.u./TZ	−397.5
SDT15_20 a.u./TZ	−399.9
SDT15_50 a.u/TZ	−399.6
SDTQ15_2 a.u./TZ	−388.4
SDTQ15_4 a.u./TZ	−390.8
SDT15_10 a.u./QZ	−397.2
SDT15_20 a.u./QZ	−398.2
SDT15_50 a.u./QZ	−399.5
Exp.[29]	−374.137661(3)

IV. CONCLUSION AND OUTLOOK

In the present paper an accurate method for the calculation of atomic electronic electric quadrupole moments is presented. The applications to the Be atom and to the Ra^+ ion demonstrate the reliability of the method.

The quadrupole shift is identified as one of the contributors to the uncertainty budget for a Tm optical clock using its ground-state fine-structure components [28], albeit not the leading one at the moment. An elaborate, detailed, and high-level study on the Tm atom in the present work shows that the EQM in its $^2F_{7/2}(4f^{13}\,6s^2)$ ground state is exceptionally small. Thus, the application of methods for systematic cancellation or suppression of the quadrupole shift [30,31] may not be necessary in a thulium optical clock.

On the methodological side the present work is motivated by the general importance of electric multipole moments and electric transition multipole moments in many areas of atomic and molecular physics. The author has also implemented $E1$ and $E2$ transition moments into the present relativistic correlated many-body methods, applications of which will be the subject of publications in the very near future. $E1$ transition moments allow for the calculation of atomic dispersion coefficients which contribute to a clock's uncertainty through the van der Waals interaction. $E2$ transition moments are of importance, for instance, in the field of parity nonconservation [32].

[1] M. S. Safronova, D. Budker, D. DeMille, D. F. Jackson Kimball, A. Derevianko, and C. W. Clark, Search for new physics with atoms and molecules, Rev. Mod. Phys. **90**, 025008 (2018).

[2] A. D. Ludlow, M. M. Boyd, J. Ye, E. Peik, and P. O. Schmidt, Optical atomic clocks, Rev. Mod. Phys. **87**, 637 (2015).

[3] A. Kozlov, V. A. Dzuba, and V. V. Flambaum, Prospects of building optical atomic clocks using Er I or Er III, Phys. Rev. A **88**, 032509 (2013).

[4] A. A. Golovizin, D. O. Tregubov, E. S. Fedorova, D. A. Mishin, D. I. Provorchenko, K. Yu. Khabarova, V. N. Sorokin, and N. N. Kolachevsky, Simultaneous bicolor interrogation in thulium optical clock providing very low systematic frequency shifts, Nat. Commun. **12**, 5171 (2021).

[5] A. Golovizin, D. Tregubov, D. Mishin, D. Provorchenko, and N. Kolachevsky, Compact magneto-optical trap of thulium atoms for a transportable optical clock, Opt. Express **29**, 36734 (2021).

[6] E. Fedorova, A. Golovizin, D. Tregubov, D. Mishin, D. Provorchenko, V. Sorokin, K. Khabarova, and N. Kolachevsky, Simultaneous preparation of two initial clock states in a thulium optical clock, Phys. Rev. A **102**, 063114 (2020).

[7] A. Golovizin, E. Fedorova, D. Tregubov, D. Sukachev, K. Khabarova, V. Sorokin, and N. Kolachevsky, Inner-shell clock transition in atomic thulium with a small blackbody radiation shift, Nat. Commun. **10**, 1724 (2019).

[8] S. Knecht, H. J. Aa. Jensen, and T. Fleig, Large-Scale Parallel Configuration Interaction. II. Two- and four-component double-group general active space implementation with application to BiH, J. Chem. Phys. **132**, 014108 (2010).

[9] T. Fleig, H. J. Å. Jensen, J. Olsen, and L. Visscher, The generalized active space concept for the relativistic treatment of electron correlation. III: Large-scale configuration interaction and multi-configuration self-consistent-field four-component methods with application to UO_2, J. Chem. Phys. **124**, 104106 (2006).

[10] J. D. Jackson, *Klassische Elektrodynamik* (Walter de Gruyter, Berlin, New York, 1983).

[11] D. Sundholm and J. Olsen, Finite-element multiconfiguration Hartree-Fock calculations of the atomic quadrupole moments of excited states of Be, Al, In, Ne, Ar, Kr, and Xe, Phys. Rev. A **47**, 2672 (1993).

[12] W. Itano, Quadrupole moments and hyperfine constants of metastable states of Ca^+, Sr^+, Ba^+, Yb^+, Hg^+, and Au, Phys. Rev. A **73**, 022510 (2006).

[13] T. Fleig, J. Olsen, and C. M. Marian, The generalized active space concept for the relativistic treatment of electron correlation. I. Kramers-restricted two-component configuration interaction, J. Chem. Phys. **114**, 4775 (2001).

[14] T. Fleig, J. Olsen, and L. Visscher, The generalized active space concept for the relativistic treatment of electron correlation. II: Large-scale configuration interaction implementation based on relativistic 2- and 4-spinors and its application, J. Chem. Phys. **119**, 2963 (2003).

[15] T. Saue, R. Bast, A. S. P. Gomes, H. J. Aa. Jensen, L. Visscher, I. A. Aucar, R. Di Remigio, K. G. Dyall, E. Eliav, E. Fasshauer, T. Fleig, L. Halbert, E. Donovan Hedegård, B. Helmich-Paris, M. Iliaš, C. R. Jacob, S. Knecht, J. K. Laerdahl, M. L. Vidal, M. K. Nayak, M. Olejniczak, J. M. Haugaard Olsen, M. Pernpointner, B. Senjean, A. Shee, A. Sunaga, and J. N. P. van Stralen, The DIRAC code for relativistic molecular calculations, J. Chem. Phys. **152**, 204104 (2020).

[16] S. Knecht, Parallel relativistic multiconfiguration methods: New powerful tools for heavy-element electronic-structure studies, Ph.D. thesis, Heinrich-Heine-Universität Düsseldorf, Düsseldorf, Germany, 2009.

[17] E. Wigner, *Group Theory and Its Applications to the Quantum Mechanics of Atomic Spectra (English Version)* (Academic, New York, 1959).

[18] M. Weissbluth, *Atoms and Molecules* (Academic, New York, 1978).

[19] T. Fleig and M. K. Nayak, Electron electric dipole moment and hyperfine interaction constants for ThO, J. Mol. Spectrosc. **300**, 16 (2014).

[20] T. Fleig and L. V. Skripnikov, P, T-Violating and Magnetic Hyperfine Interactions in Atomic Thallium, Symmetry **12**, 498 (2020).

[21] B. P. Pritchard, D. Altarawy, B. Didier, T. D. Gibson, and T. L. Windus, A New Basis Set Exchange: An Open, Up-to-date Resource for the Molecular Sciences Community, J. Chem. Inf. Model. **59**, 4814 (2019).

[22] K. G. Dyall, Relativistic double-zeta, triple-zeta, and quadruple-zeta basis sets for the 4s, 5s, 6s, and 7s elements, J. Phys. Chem. A **113**, 12638 (2009); Basis sets available from the Dirac web site, http://dirac.chem.sdu.dk.

[23] R. Pal, D. Jiang, M. S. Safronova, and U. I. Safronova, Calculation of parity-nonconserving amplitude and other properties of Ra^+, Phys. Rev. A **79**, 062505 (2009).

[24] B. K. Sahoo, B. P. Das, R. K. Chaudhuri, D. Mukherjee, R. G. E. Timmermans, and K. Jungmann, Investigations of Ra^+ properties to test possibilities of new optical frequency standards, Phys. Rev. A **76**, 040504(R) (2007).

[25] A. Kramida, Yu. Ralchenko, J. Reader, and NIST ASD Team, NIST Atomic Spectra Database (ver. 5.9). Available: https://physics.nist.gov/asd [2022, May 21]. National Institute of Standards and Technology, Gaithersburg, MD., 2021.

[26] D. Jiang, B. Arora, and M. S. Safronova, Electric quadrupole moments of metastable states of Ca^+, Sr^+, and Ba^+, Phys. Rev. A **78**, 022514 (2008).

[27] A. S. P. Gomes, L. Visscher, and K. G. Dyall, Relativistic double-zeta, triple-zeta, and quadruple-zeta basis sets for the lanthanides La–Lu, Theor. Chem. Acc. **127**, 369 (2010).

[28] D. Sukachev, S. Fedorov, I. Tolstikhina, D. Tregubov, E. Kalganova, G. Vishnyakova, A. Golovizin, N. Kolachevsky, E. Kharabova, and V. Sorokin, Inner-shell magnetic-dipole transition in Tm atoms: A candidate for optical lattice clocks, Phys. Rev. A **94**, 022512 (2016).

[29] D. Giglberger and S. Penselin, Ground-state hyperfine structure and nuclear magnetic moment of thulium-169, Z. Phys. **199**, 244 (1967).

[30] W. Oskay, W. M. Itano, and J. Bergquist, Measurement of the $^{199}Hg^+$ $5d^9 6s^2\,{}^2D_{5/2}$ Electric Quadrupole Moment and a Constraint on the Quadrupole Shift, Phys. Rev. Lett. **94**, 163001 (2005).

[31] P. Dubé, A. A. Madej, J. E. Bernard, L. Marmet, J.-S. Boulanger, and S. Cundy, Electric Quadrupole Shift Cancellation in Single-Ion Optical Frequency Standards, Phys. Rev. Lett. **95**, 033001 (2005).

[32] N. Fortson, Possibility of Measuring Parity Nonconservation with a Single Trapped Atomic Ion, Phys. Rev. Lett. **70**, 2383 (1993).